



DIE ERDE

Journal of the  
Geographical Society  
of Berlin

# Mitigation of urban heat stress – a modelling case study for the area of Stuttgart

Joachim Fallmann<sup>1</sup>, Stefan Emeis<sup>1</sup>, Peter Suppan<sup>1</sup>

<sup>1</sup> Institute for Meteorology and Climate Research (IMK-IFU) of the Karlsruhe Institute of Technology (KIT), Kreuzackbahnstr. 19, 82467 Garmisch-Partenkirchen, Germany, joachim.fallmann@kit.edu, stefan.emeis@kit.edu, peter.suppan@kit.edu

Manuscript submitted: 18 June 2013 / Accepted for publication: 26 August 2013 / Published online: 28 April 2014

## Abstract

In 2050 the fraction of urban global population will increase to over 69 %, which means that around 6.3 billion people are expected to live in urban areas (UN 2011). Cities are the predominant habitation places for humans to live and are vulnerable to extreme weather events aggravating phenomena like heat stress. Finding mitigation strategies to sustain future development is of great importance, given expected influences on human health. In this study, the mesoscale numerical model WRF is used on a regional scale for the urban area of Stuttgart, to simulate the effect of urban planning strategies on dynamical processes affecting urban climate. After comparing two urban parameterisation schemes, a sensitivity study for different scenarios is performed; it shows that a change of the reflective properties of surfaces has the highest impact on near-surface temperatures compared to an increase of urban green areas or a decrease of building density. The Urban Heat Island (UHI) describes the temperature difference between urban and rural temperatures; it characterises regional urban climate and is responsible for urban-rural circulation patterns. Applying urban planning measures may decrease the intensity of the UHI in the study area by up to 2 °C by using heat-reflective roof paints or by 1 °C through replacing impervious surfaces by natural vegetation in the urban vicinity – compared to a value of 2.5 °C for the base case. Because of its topographical location in a valley and the overall high temperatures in this region, the area of Stuttgart suffers from heat stress to a comparatively large extent.

## Zusammenfassung

Laut Berechnungen der Vereinten Nationen werden bis zum Jahr 2050 69 % aller Menschen in Städten leben, das entspricht ca. 6,3 Milliarden (UN 2011). Städte sind damit der wichtigste Lebensraum für Menschen. Sie reagieren besonders sensibel auf Extremwetterereignisse wie zum Beispiel Hitzewellen, die die Wärmebelastung für die Bewohner verschärfen. Um nachhaltig negativen Auswirkungen auf die menschliche Gesundheit vorzubeugen, sind Anpassungs- und Vermeidungsstrategien notwendig. In dieser Studie wird das mesoskalige numerische Strömungs-Simulationsmodell WRF verwendet, um für das Stadtgebiet Stuttgart auf regionalem Maßstab Szenarienrechnungen durchzuführen. Damit sollen die Auswirkungen verschiedener Stadtplanungsmaßnahmen auf dynamische Prozesse im Stadtklima qualitativ und quantitativ untersucht werden, und die Wirksamkeit der einzelnen Strategien soll bewertet werden. Nach dem Vergleich zweier Parametrisierungsansätze für städtische Gebiete im Modell wird eine Sensitivitätsanalyse durchgeführt; diese zeigt, dass eine Veränderung der Reflexionseigenschaften von Oberflächen, verglichen mit Begrünung oder Veränderung der Bebauungsdichte, den größten Einfluss auf bodennahe Lufttemperaturen hat. Der Begriff ‚städtische Wärmeinsel‘ (engl. Urban Heat Island UHI) beschreibt den Unterschied zwischen

Fallmann, Joachim, Stefan Emeis and Peter Suppan 2013: Mitigation of urban heat stress – a modelling case study for the area of Stuttgart. – DIE ERDE 144 (3-4): 202-216



DOI: 10.12854/erde-144-15

städtischer und ländlicher Temperatur, ist verantwortlich für die Ausprägung von regionalen Strömungsmustern und charakterisiert so das städtische Klima. Laut Modellergebnis kann durch die Verwendung von stark reflektierenden Materialien oder Außenanstrichen die Intensität der Wärmeinsel um bis zu 2 °C herabgesetzt werden, wohingegen innerstädtische Grünflächen die Temperaturdifferenz zwischen Stadt und Umland im Mittel um 1 °C verringern können.

**Keywords** Urban Heat Island, heat stress, WRF urban, mitigation strategies, Stuttgart, Germany

## 1. Introduction

Through the rapid growth of cities all over the world, public awareness for the local-climatic phenomenon of the Urban Heat Island (UHI) has increased during the past decades, in research, economics, urban planning and society.

UHI describes the tendency for an urbanised area, because of its radiative and geometrical features, to get warmer than its rural surroundings, generating its own microclimate (Oke 1982). Low-albedo materials of impervious surfaces like pavements, roads and roofs absorb the bulk of the incoming solar radiation and re-radiate in the infrared (Taha 1997). The annual mean temperature of the central areas of a large city is about 1 ° to 3 °C higher than in the surrounding areas, and in individual calm clear nights the actual temperature can be as much as 12 °C higher (Oke 1982). The difference between urban and rural (surface) temperature is defined as Urban Heat Island Intensity (UHII) and can be retrieved from satellite data or by comparing observed or modelled near-surface temperatures at specific locations within and in the surroundings of the urban area.

Additional heat generated by fuel combustion, air conditioning or other human activities as well as roughness effects caused by building structures help to 'design' specific atmospheric dynamics resulting in modified urban-rural circulation patterns (Arnfield 2003). In addition to health problems produced by rising temperatures, accelerating photochemical reaction rates can worsen the inner-city air quality (United States Environmental Protection Agency (EPA) 2008).

Results by Poumadère et al. (2005) suggest that climate change could have been responsible for the European Heat Wave 2003. This was the warmest and driest summer since 1500 AD, which caused over 30,000 heat-related deaths in Europe, especially in its western part.

When the human body is no longer able to cope with excessive exposure to temperature extremes during heat waves, it loses its ability to cool down and results

can be dehydration or circulatory collapse, which can result in death. Especially older or medically handicapped people and babies suffer from heat stress and thus are very vulnerable to urban climate extremes. Hyperthermia or thermal stress are analogous terms (Poumadère et al. 2005; Lubber and McGeehin 2008). The urban heat island phenomenon accounts for an amplification of these risks, which underlines the importance of mitigation strategies.

Specific urban planning strategies, like green roofs or facades and highly reflective materials are able to reduce the UHI. Taha (1997) demonstrated that increasing the albedo by 0.15 can reduce peak summertime temperatures for the urban area of Los Angeles by up to 1.5 °C. During the DESIREX Campaign 2008, Salamanca et al. (2012) stated that a higher albedo leads to about 5 % reduction in energy consumption through air conditioning during summertime periods for the area of Madrid. Solecki et al. (2005) studied extensively the effect of urban vegetation in New Jersey, whereas Onishi et al. (2010) evaluated the potential for UHI mitigation by greening parking lots in the city of Nagoya, Japan. The regional energy saving effect of high-albedo roofs can also be found in Akbari et al. (1997) and a more global perspective in Akbari et al. (2009) and Oleson et al. (2010). Zhou and Shepherd (2010) investigated the UHI of Atlanta under extreme heat conditions and stated that an increasing vegetation fraction and evapotranspiration were the most effective mitigation strategies for that area.

In the current study, the numerical mesoscale Weather Research and Forecasting Model WRF 3.4 (Skamarock et al. 2005) is used to analyse the urban climate on a regional scale. This analysis allows an assessment of UHI mitigation strategies through simulating different urban planning scenarios. Different parameterisation schemes are available in WRF for representing urban surfaces and the way the urban canopy affects dynamical processes in the lower atmosphere (Chen et al. 2011).

The work is part of the EU-Project 3CE292P3 'UHI – Development and application of mitigation and adap-

tation strategies and measures for counteracting the global UHI phenomenon' and focuses on the metropolitan area of Stuttgart in the south-western part of Germany. Due to Stuttgart's geographical location in a valley, the weak mountain-valley circulation leads to an increasing potential for natural heat trapping in the urban region. This is especially true during heat waves and stable weather conditions of high pressure systems with less pronounced winds and low air exchange rates. Since Stuttgart is well-equipped with meteorological measurement stations, and as one of the warmest regions in Germany, it is well suited for conducting urban climate studies. According to modelling work of the Department for Urban Climate (Office for Environmental Protection Stuttgart), the area of the city with heat stress on more than 30 days/year is anticipated to increase from 6 % (in 1971-2000) to 57 % (in 2071-2100), using the SRES A1B IPCC Emission Scenario (Amt für Umweltschutz Stuttgart 2013).

Several parameterisation schemes are tested to represent the metropolitan region of Stuttgart and its interaction with the surrounding environment in the mesoscale model WRF. Results are compared against observation data. In addition, various urban planning strategies are examined, namely: enhancing the reflective properties of buildings by using light colours for roof and wall surfaces; introducing green areas replacing impervious surfaces; and altering geometrical features by decreasing the building density. The first two strategies are likely to cool down the surface temperature either by reflecting radiation or through increased evapotranspiration (Taha 1997). Reducing the building density enhances the circulation of air within street canyons. In the final section different

scenarios are discussed and analysed in an attempt to quantify the impact of each strategy.

Results from this work can offer decision support to local authorities for a sustainable urban development and contribute to climate research through improved models dealing with urban environments.

2. Methodology

2.1 Area of interest

Stuttgart, located in the south-western part of Germany, is the capital of the federal state of Baden-Württemberg. With around 600,000 inhabitants, it is the centre of a metropolitan region of about 2.7 mill. people. The city is located in a valley, with a difference of elevation between city centre and surrounding hills of about 150-200 m. The climate of Stuttgart is characterised by a large number of days of sunshine and mild weather with weak winds generally from the south-west. At low elevation in the Neckar basin, the greater Stuttgart region is one of the warmest areas of Germany. Observations at the inner-city meteorological station Stuttgart Low Schwabenzentrum show an annual mean air temperature of 10 °C, a mean wind speed of 2 m/s and an average annual precipitation of 573 mm. The average July temperature is 18 °C and maximum July temperatures exceed 37 °C. The Stuttgart metropolitan area covers approximately 200 km<sup>2</sup>, with about 42 % impervious urban land surface (Amt für Umweltschutz Stuttgart 2013). Low wind speed throughout the year leads to weak air mixing. During stable weather conditions, weak winds in the valley result in a strong trapping in-

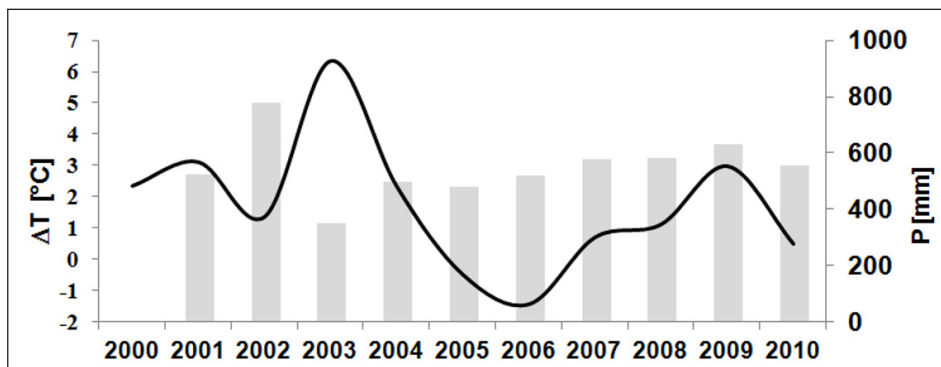


Fig. 1 2-m-temperature difference from the annual average 1961-1990 (solid line) and yearly-accumulated rainfall (bars) for the measurement station Stuttgart Schwabenzentrum in the city centre, 2000-2010, showing the year 2003 as the warmest and driest in recent climate history. The extreme 2003 temperatures are mostly the result of the heat wave of July and August 2003 (Amt für Umweltschutz Stuttgart 2013)

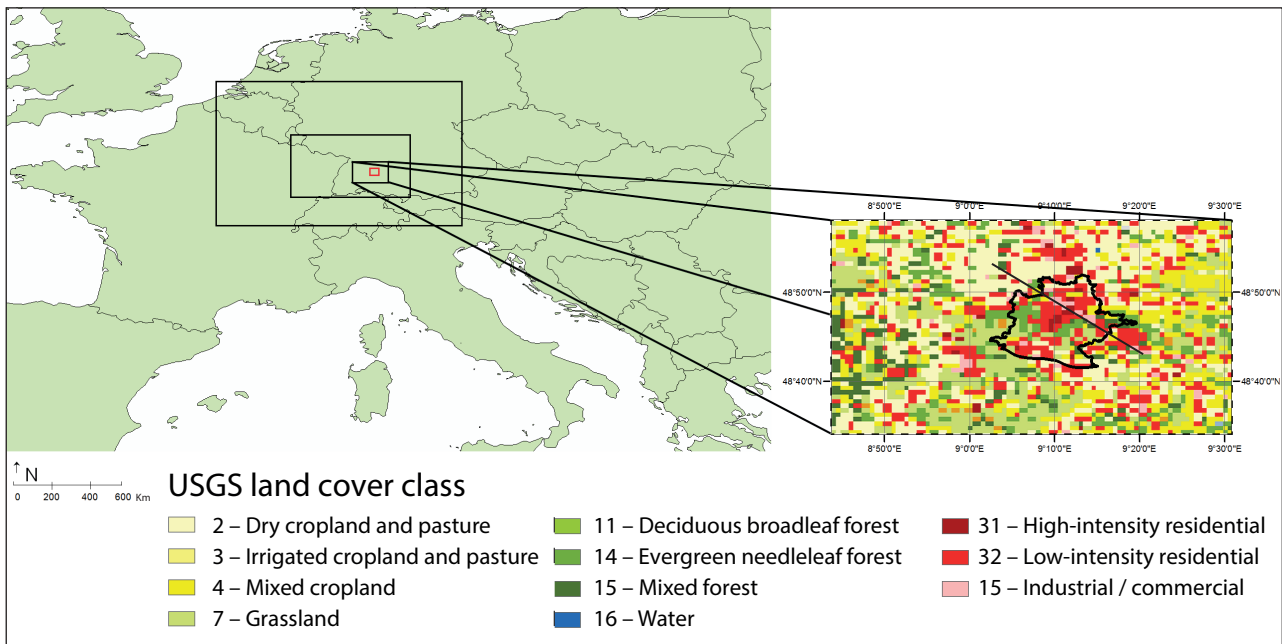


Fig. 2 Location of modelling domains (left) (Source: map adapted from Sandvik 2009) and urban area of Stuttgart, equal to size of domain 3 (right) representing an area of 61 x 49 km, and USGS classified land cover with 1 km resolution (United States Environmental Protection Agency (EPA) 2008). The diagonal line represents the cross-section used for further studies.

version and pollutants remain over and within the urban area. Stable weather patterns associated with high pressure ridges produce high temperatures harmful to human health together with periods with poor air quality (Amt für Umweltschutz Stuttgart 2013). Observation data for Stuttgart show 2003 as the warmest and driest year within the last decade, compared to the period 1961-1990 (Fig. 1). On August 13th 2003, a temperature of 37.5 °C was recorded at 17:00 h in the inner city and on August 17th evening temperatures remained at 25 °C in combination with a relative humidity of 82 % (Amt für Umweltschutz Stuttgart 2013). This aggravated the effect of heat stress.

The difference between urban and rural temperature, expressed as UHI, is dominated by a location's topographical and meteorological situation. In the case of Stuttgart, the winds are often very weak or blocked by natural obstacles, which aggravates UHI formation. Looking at the near-surface temperature and 10-metre wind speed observations for a summer day in the year 2003, there are distinct differences between an urbanised station in the centre and a site at the more rural outskirts towards the south-east (Location Hohenheim). The period August 11-18 2003 shows an average temperature difference of 1.3 °C, with maxima reaching about 4 °C in evening and night time hours and winds of 0.8 m/s for the

urban area and 2.3 m/s for the rural location. (Locations of both stations are given in Figure 4.)

Urban climatology records have been available for Stuttgart since 1935. A major element of Stuttgart's climate is the weak wind, and the orography makes it nearly impossible to draw a consistent wind rose for the whole area of Stuttgart. Regulating the spreading of pollutants, wind speed plays a decisive role for air hygiene and, with the only real opening of the valley to the northeast along the Nesenbach stream, mixing of air masses is very weak. The combination of regional high temperatures and high humidity turns the area into a region with considerable danger of heat stress. To offset these natural disadvantages, it is of great importance to initiate measures for a sustainable and energy-saving urban land-use planning for future projects (Amt für Umweltschutz Stuttgart 2013).

## 2.2 Modelling approach

For the numerical study a time period with only small changes in weather conditions and comparatively high air temperatures was chosen. The period between August 11th and August 18th 2003 coincided with an extreme heat wave across Europe (Poumadère et al. 2005). Low wind speeds meant weak circulation

Tab. 1 Configuration of WRF settings

Geographical input data	1 km USGS land use
dx, dy	15 km, 3 km, 1 km
West-east [km]	645, 228, 61
South-north [km]	510, 168, 49
Vertical layers	36
Lowest model level	15 m
Meteorological BC	0.5 Deg ERA-Interim
Start time	8/11/03 – 0:00 UTC
End time	8/18/03 – 0:00 UTC
Microphysics	WSM06 (Hong)
Longwave	RRTM (Mlawer 1997)
Shortwave	Goddard (Chou 1994)
Urbanisation scheme	BEP
Land surface model	Noah LSM
Cumulus scheme	Kain-Fritsch (2004)
Boundary layer	MYJ

of air, and the constantly high humidity aggravated the phenomenon of heat stress even more.

The initial conditions were obtained from ECMWF ERA Interim 0.5° resolution reanalysis data (ECMWF 2013). The model uses 3 domains in a two-way interactive nesting approach. The innermost domain covers the entire urban area of Stuttgart and the closest rural surroundings, an area of approximately 3000 km<sup>2</sup>. Down-scaling techniques and nesting allow a resolution down to 1 km. Table 1 indicates the basic settings of WRF.

The basic 24-class USGS classification used in WRF is modified using information from 33-class CORINE

land-use data in such a way that the ‘urban’ classified grid cells are separated into 3 different groups, i.e. the new urban categories high-density residential, low-density residential and industrial/commercial (Fig. 2). The 3 urban classes are distinguished based on their appearance and percentage of impervious surface. Low-intensity residential (class 31) includes areas with a mixture of built-up plots and vegetation, with vegetation accounting for 20-70 % of the land cover. In contrast, vegetation is under 20 % for high-density residential areas (class 32). Industrial/commercial (class 33) includes infrastructure and highly developed areas not classified as residential (USGS 2006). GIS techniques made it possible to resample 250 m resolution CORINE data to the 1 km USGS land-use classification grid, which was then transferred back to the WRF geographical input database.

In the Stuttgart metropolitan area, 41 % of the model domain for the innermost nest is defined as urban; 80 % is low-density residential, 7 % high-density residential and the remaining 13 % industrial/commercial.

The basic WRF model settings have to be changed and adapted for this case, especially to accommodate the new land use information. For microphysics, the Single-Moment 6-class scheme is applied, for shortwave radiation the Goddard and for long wave radiation the RRTM scheme is used (Tab.1). The simulations use 36 vertical levels, with the lowest model level located at 12 m above ground. The WRF 2-metre potential temperature used throughout the study is approximated from the vertical temperature distribution. The Kain-Fritsch cumulus parameterisation (Kain 2004) is applied only to the coarsest domain and is turned off for the inner two nested domains. The resolution of the geographical input data is 30'' (about

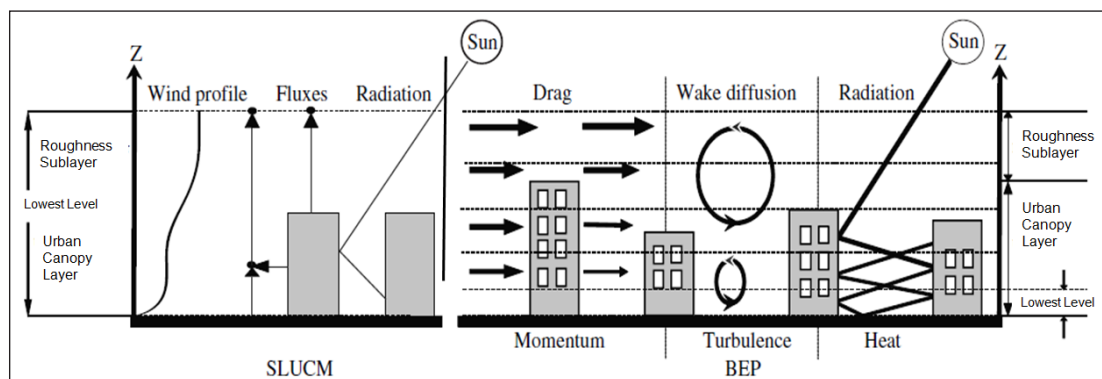


Fig. 3 Schematic figure of Single Layer Urban Canopy Model (Kusaka et al. 2001) (left) and multi-layer model: Building Effect Parameterisation (Martilli et al. 2002) right. These differ in representing the processes in the urban canopy layer (Chen et al. 2011).

1 km) and of meteorological data 0.5° (about 50 km). For calculating the planetary boundary layer, the Mellor-Yamada-Jancic – MYJ (Janjic 1994) approach is chosen, because it gives high vertical resolutions and best represents the turbulent kinetic energy term in a multi layer urban canopy model (Martilli et al. 2002).

To represent different types of land surfaces and their interaction with the lower atmosphere, WRF is coupled with the NOAH Land Surface Model – LSM (Mitchell 2005), which numerically calculates relevant physical processes at each grid cell. Land cover information helps to account for properties of different land surfaces whereas the three-dimensional structure of urban areas which directly interacts with the lowest model layer is represented by specific urban parameters. For WRF, there are 4 different urban parameterisation schemes available: a bulk urban parameterisation (Liu et al. 2006) which uses characteristic properties of urban surfaces without distinguishing between different urban canopy layers, geometrical features or heat transfer of urban structures like buildings and roads; a single layer approach (Kusaka et al. 2001); a multi layer approach (Martilli et al. 2002); as well as a multi layer model accounting for indoor-outdoor heat exchange (Salamanca et al. 2010). Three of these are tested for their ability to model the effect of urban surfaces on local climate and circulation patterns. Generally, there is a simpler Single-Layer Urban Canopy Model (SLUCM) and a more specific multi-layer approach called Building Effect Parameterisation BEP (Chen et al. 2011). Schematic diagrams of both schemes are shown in Figure 3.

The SLUCM (Kusaka et al. 2001) assumes infinitely long street canyons, representing shadowing, reflection and radiation trapping in the street canyon and specifies an exponential wind profile. Temperatures of urban surfaces are calculated from surface energy budgets and thermal conduction equations. The surface-sensible heat flux is computed by using Monin-Obukhov similarity theory. Canyon drag coefficient and friction velocity is approximated by a similarity stability function for momentum. SLUCM uses about 20 parameters which are adapted to the urban area of interest (Chen et al. 2011).

The Building Effect Parameterisation approach BEP (Martilli et al. 2002) accounts for the three-dimensional nature of urban surfaces and treats the buildings as sources and sinks of heat, moisture and momentum. Impacting the thermodynamic struc-

ture of the urban roughness sub-layer in the lower part of the urban boundary layer, BEP allows a direct interaction with the PBL. Effects of horizontal and vertical surfaces on turbulent kinetic energy (TKE), potential temperature ( $\Theta$ ) and momentum are also covered by this model, allowing a high vertical resolution close to the ground. For these simulations, the internal temperature of the buildings is assumed to be constant (Chen et al. 2011).

The bulk approach where urban canopy parameterisation is turned off is used for the sensitivity study, whereas the BEM approach is not used here.

For each urban class, parameters are defined to represent urban properties (e.g. building height, street width, surface albedo or vegetation cover), accounting for building and street orientation, as well as thermodynamic properties and roughness features (Tab. 2). To determine the mean building height for each urban class, a high-resolution digital elevation model from the land surveying office Stuttgart is used, resolving the height of every building in the urban area. Orientation and mean width of roads are calculated from Google Maps using ArcGIS 10.1 software. Anthropogenic heat and other listed parameters are included by estimated values currently used in the latest version of WRF (Chen et al. 2011).

The total sensible heat flux from an urban classified grid cell is calculated on the basis of these parameters and is used by the NOAH LSM to calculate land surface properties. For each grid cell, the simulation uses a 1 km<sup>2</sup> mean-value. Based on a sensitivity study, it is decided which urban parameterisation approach is most suitable for the model performance.

### 3. Results

#### 3.1 Sensitivity to urban parameterisations

The simulation results are to be compared against observation data, to test the ability of the urban canopy model to reproduce basic meteorological variables. Two retrospective simulations were made for the period August 11-18 2003, in which the urban parameterisation schemes were varied. Comparisons between the simulated and observed 2 m potential temperature for both approaches are shown in the following figures. Potential temperature was selected for the comparison to remove elevation dependence.

Tab. 2 Urban parameters as input to the urban parameterisation scheme; Parameters are derived for the three CORINE-based urban classes: high-density residential, low-density residential and commercial. The lower part of the table is only valid for the BEP approach, representing the distribution of the buildings with regard to height and street characteristics for each class (adapted from Chen et al. 2011)

Urban parameter	Commercial	High-density	Low-density
ZR: roof level (building height) [m]	8.5	9.7	6.4
SIGMA_ZED: standard deviation of roof height [m]	6.8	6.4	4.5
ROOF_WIDTH: roof (i.e. building) width [m]	27.5	13.3	10
ROAD_WIDTH: road width [m]	19	16.2	18
AH: Anthropogenic heat [W m <sup>2</sup> ]	90	50	20
FRC_URB: Fraction of the urban landscape without natural vegetation [fraction]	0.95	0.85	0.5
CAPR: Heat capacity of roof [J m <sup>3</sup> /K]	1.00E+06	1.00E+06	1.00E+06
CAPB: Heat capacity of building wall [J m <sup>3</sup> /K]	1.00E+06	1.00E+06	1.00E+06
CAPG: Heat capacity of ground (road) [J m <sup>3</sup> /K]	1.40E+06	1.40E+06	1.40E+06
AKSR: Thermal conductivity of roof [J/ m s K]	0.67	0.67	0.67
AKSB: Thermal conductivity of building wall [J/m s K]	0.67	0.67	0.67
AKSG: Thermal conductivity of ground (road) [J/m s K]	0.4	0.4	0.4
ALBR: Surface albedo of roof [fraction]	0.2	0.2	0.2
ALBB: Surface albedo of building wall [fraction]	0.2	0.2	0.2
ALBG: Surface albedo of ground (road) [fraction]	0.2	0.2	0.2
EPSR: Surface emissivity of roof [-]	0.8	0.9	0.93
EPSB: Surface emissivity of building wall [-]	0.8	0.95	0.94
EPSG: Surface emissivity of ground (road) [-]	0.95	0.96	0.97
ZOB: Roughness length for momentum, over building wall [m]	0.0001	0.0001	0.0001
ZOG: Roughness length for momentum, over ground (road) [m]	0.01	0.01	0.01
ZOR: Roughness length for momentum over roof [m]	0.01	0.01	0.01
AKANDA_URBAN: Coefficient modifying the Kanda approach to computing surface layer exchange coefficient	1.29	1.29	1.29
TBLEND: Lower boundary temperature for building wall temperature [ K ]	293	293	293
TGLEND: Lower boundary temperature for ground (road) temperature [ K ]	293	293	293

Only BEP:

Street parameters				Building heights			
Urban category [index]	Street direction [deg from N]	Street width [m]	Building width [m]	Height [m]	Category 1 [%]	Category 2 [%]	Category 3 [%]
1	0	19	25	5	44	33	48
1	90	19	25	10	26	20	37
2	0	15	13	15	14	23	11
2	90	15	13	20	8	18	3
3	0	18	10	25	4	4	1
3	90	18	10	30	2	2	-
				35	2	-	-

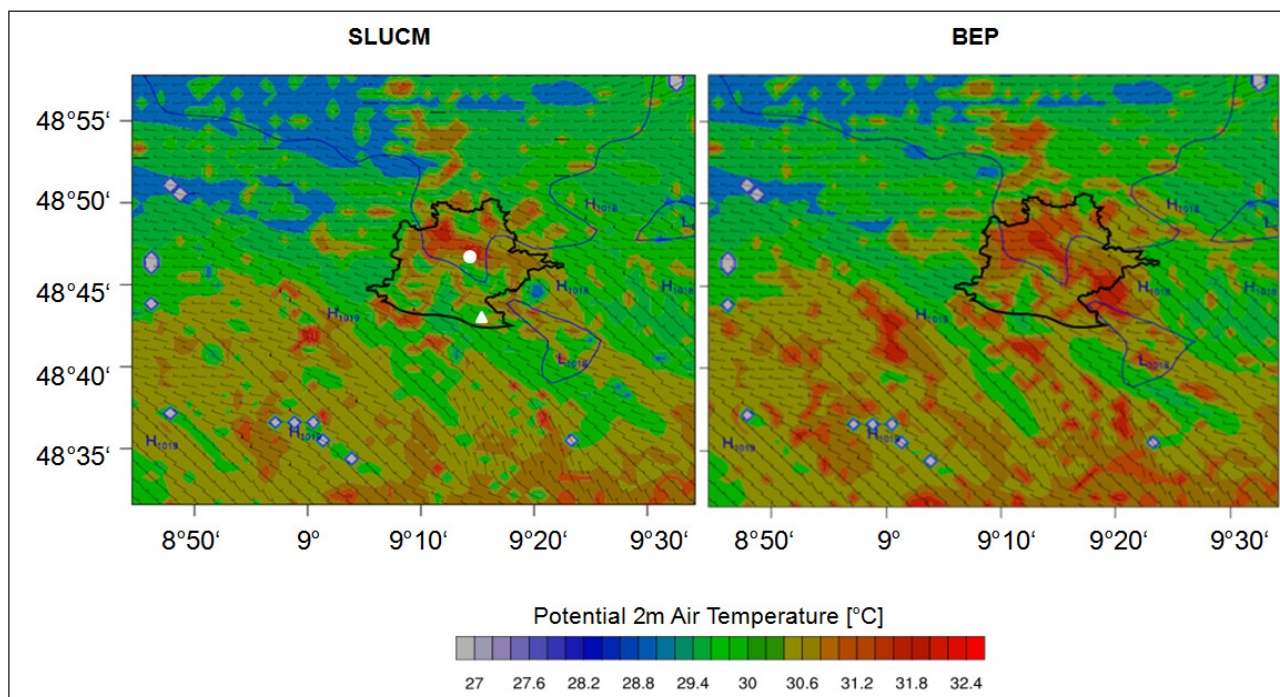


Fig. 4 2 m potential temperatures modelled with single layer model (SLUCM, left) and multi-layer approach (BEP, right) for the period August 11-18 2003; selection of August 13, 2003 18:00 UTC. The area shows modelling domain 3. Slight black lines indicate isobars, the black shape is the urban area of Stuttgart, the white dot is the urban measurement station 'Stuttgart Schwabenzentrum', the white triangle shows the more rural station 'Stuttgart Hohenheim' about 8 km away from the city centre.

Figure 4 shows the potential temperature fields for both simulations at 1800 UTC (2000 local time) on August 13 2013. This point in time was chosen because it is considered that most of the heat at that time had been generated by the interaction between urban surface and solar radiation throughout the day. Through absorption processes, the heat is stored in the impervious materials or remains in the street canyon. The rural surrounding has already started to cool down, while the urban area still remains warmer. The Urban Heat Island effect is most distinct in the evening hours and lasts through the night and early morning (Oke 1982). Both parameterisation schemes produce a maximum potential temperature of over 305 K (32 °C), but for the BEP approach (right), higher temperatures are reached more often throughout the urban area. Overall, the multi-layer model tends to reproduce the higher temperatures better than the single-layer approach.

The difficulty in comparing modelling results with measurement data is that the fixed location of the measurement station is assumed to be representative of a 1 x 1 km grid cell. The hourly output for the 7 days of simulation is plotted against the observed measurements to test the ability of the parameterisation scheme to reproduce extreme events. A third

run is conducted for only bulk urban parameterisation (Liu et al. 2006) to examine whether an urban parameterisation scheme improves the simulation result. Scatter plots are shown in Figure 5.

The BEP approach shows the highest correlation to the observed potential temperature ( $R^2 = 0.71$ ), the SLUCM approach shows a reduction in the correlation coefficient by 7 %, while no urban parameterisation gives a 15 % decrease. The separation of night-time and day-time scatter plots reveals a slightly better correlation for the nightly temperatures ( $R^2 = 0.62$ ) compared to the daily ones ( $R^2 = 0.53$ ). This might be due to an additional problem caused by incoming direct solar radiation.

Surface wind speed (1-3 m/s) for the simulated period is very low and the model has difficulties reproducing small changes in the flow. Looking at the diurnal development of wind speed, again the BEP approach seems best suited for characterising this parameter (Fig.6).

The results from the sensitivity study suggest that the BEP approach is more suitable for conducting UHI mitigation scenarios with the WRF model for this case. In the following section the simulations

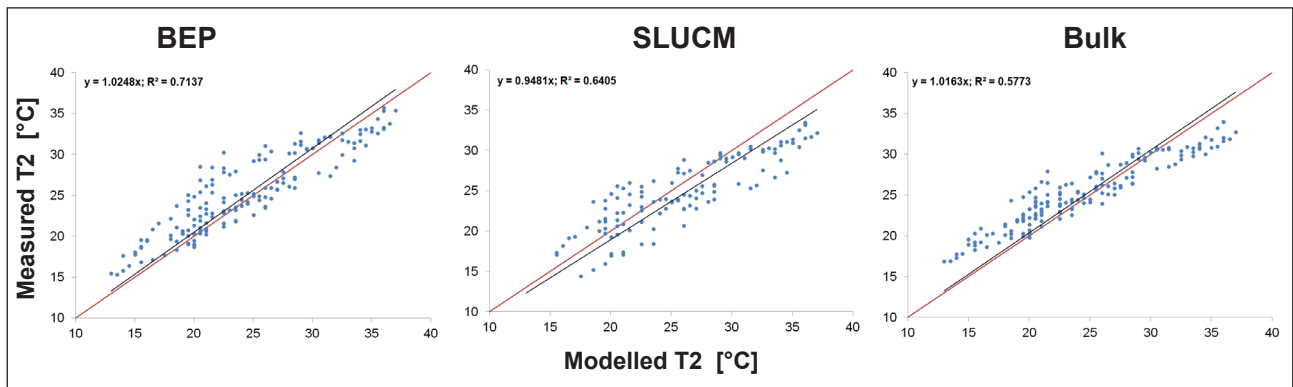


Fig. 5 Observations compared with modelled temperature for each parameterisation scheme: Building Effect Parameterisation BEP (Martilli et al. 2002), Single-Layer Urban Canopy Model SLUCM (Kusaka et al. 2001) and Bulk Approach (Liu et al. 2006). The location of the measurement station is indicated by a white dot in Figure 4.

will be expanded to examine the impact of urban planning strategies on UHI formation. First, the ability of green surfaces to cool down the near-surface temperature through evaporation processes and photosynthesis will be examined. Next, we examine the alteration of reflection characteristics of impervious surfaces like building roofs and walls by increasing the surface albedo (Taha 1997). And finally, the changing of geometrical features, like building density, will be analysed. Since the wind speed is very low in this period (1-1.5 m/s), only thermal factors are considered in the results. The interaction between slope winds and UHI formation is not discussed at this point. Referring to Figure 7, August 13 shows a maximum in UHI intensity for the modelling period. The difference between urban and rural temperatures reaches a value of up to 4.5 °C at around 03:00 UTC, drops again in the

morning hours and reaches a second maximum at around 18:00 UTC (20:00 local time). Humidity during periods of high UHI intensity is lower and wind speed does not exceed 2 m/s.

### 3.2 Sensitivity to urban design

In response to extreme heat events like the one of summer 2003 portrayed here, urban planners and city authorities attempt to find mitigation scenarios to improve the living conditions for the local inhabitants. Usually city planners use green surfaces, highly reflective building materials and a changed building geometry as tools to reduce the effects of heat. The use of these planning tools will be examined in the WRF simulations. According to previous research, urban greening may considerably reduce the UHI effect

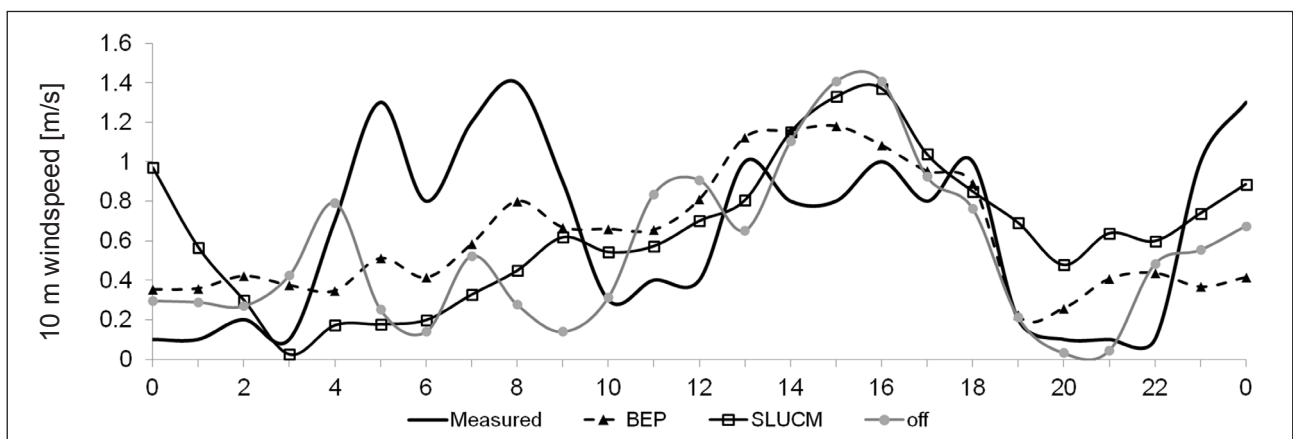


Fig. 6 Measured and simulated wind speed in the course of the day of August 13, 2003 from midnight to midnight for 3 different modelling approaches (BEP, SLUCM and bulk approach). Dashed line with triangles refers to the BEP approach used later.

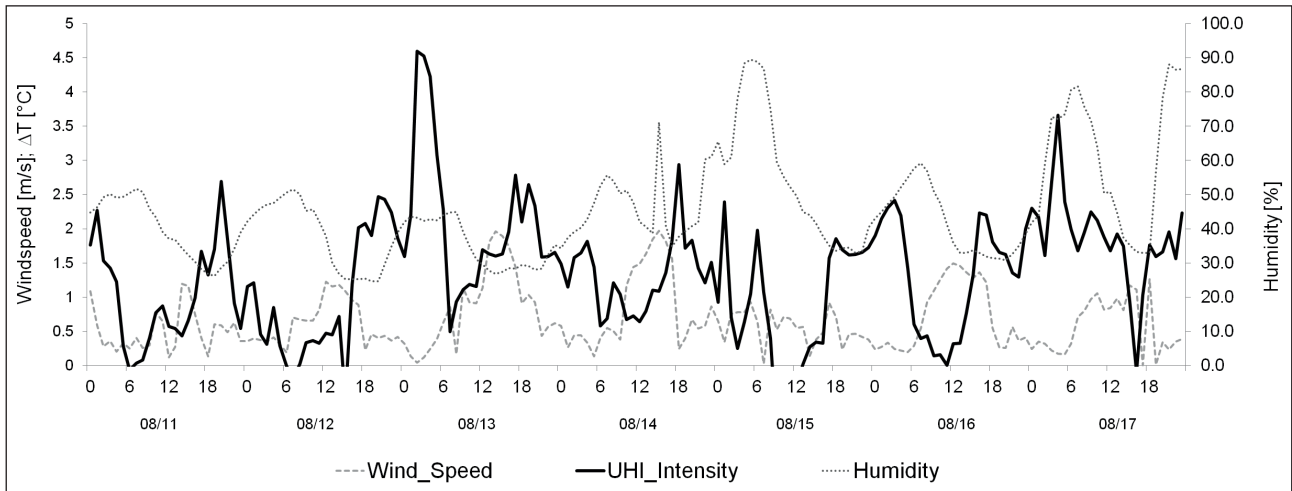


Fig. 7 Development of UHI intensity, 10 m horizontal wind speed and relative humidity for the modelling period August 11-18, 2003 using BEP approach and control case

and mitigate heat stress. This scenario will be simulated in the model by running two different ‘City Park’ simulations. The first is the ‘Central Park’ scenario where 25 grid cells classified as urban in the centre of Stuttgart are replaced by natural vegetation. This change accounts for 25 km<sup>2</sup>, or approximately 12 % of the total city area to be transferred into a park area. For the other urban greening scenario (‘Many Parks’), several smaller green areas are installed. The size of every individual park within the city borders is assumed to be equal, and their total area is the same as in the ‘Central Park’ simulation. Transformation from impervious surface into vegetation is represented by changing characteristic parameters as shown in Table 3. These modified parameters create new boundary conditions for the NOAH LSM and WRF.

Another measure to reduce near-surface temperatures is the modification of the reflective characteristics of impervious surfaces (e.g. by changing the roof colour or using highly reflecting materials). In the model this can be achieved by changing the albedo of roofs and building walls in the urban parameter table

from 0.2 to 0.7 (‘Albedo’). The third case study ‘Density’ reflects a direct intervention into the building structure. Within the urban table the proportion of roof width to road width is increased by 20 % which in turn results in a larger area being covered by natural vegetation such as trees and grassland. For all these case studies a modelling run using BEP is performed for the same period of time. The effectiveness of each scenario is indicated by the difference between modelled temperatures for scenario run and control case.

Figure 8 illustrates the difference in 2 m potential temperature ( $\theta$ ) for each urban planning strategy. The changes in  $\theta$  range from -2 to 0 °C, whereas in certain areas an increase in air temperature is registered, but only up to 0.5 °C. The areas with blue and white shading indicate a decrease of near-surface temperature. For the ‘Albedo’ scenario the reflectivity for each urban grid cell throughout the domain is modified, which results in a net temperature decrease throughout the domain. The strongest effect, i.e. the largest decrease in  $\theta$ , is in the city centre with the highest building densities. For the ‘Density’ case, the impacts are seen mostly in

Tab. 3 Changes in land surface properties after transformation from impervious to natural surface, using the most important parameters according to calculations in NOAH LSM (Mitchell 2005)

	Albedo [%]	Soil moisture [m <sup>3</sup> /m <sup>3</sup> ]	Surface emissivity	Roughness length [cm]	Vegetation fraction [%]
<b>Urban</b>	17.3	0.1	0.9	76.7	18.0
<b>Vegetation</b>	23.0	0.25	0.96	12.0	80.0

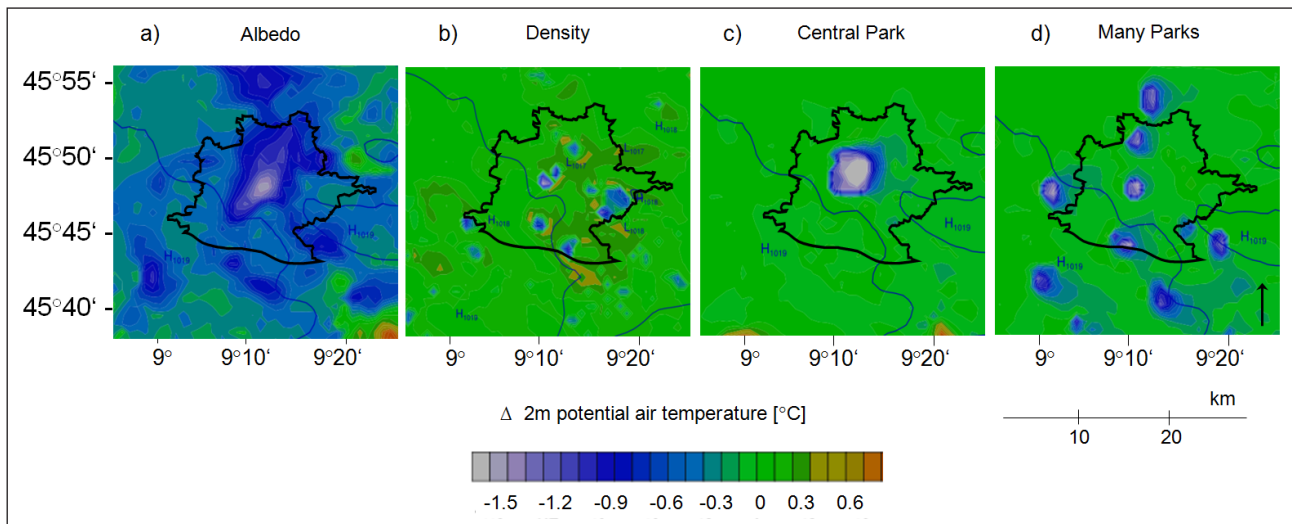


Fig. 8 Difference in potential 2 m air temperature for the four scenarios: a) changed albedo for roofs and walls, b) modified proportion street width/building height; and the two urban greening scenarios with one big park (c) and a number of smaller parks (d); projected time is August 13, 2003, 18:00 UTC

the high-density urban areas where the building geometry has the largest influence on near-surface potential temperature. To show the ability of a certain strategy to decrease UHI intensity, the averaged temperature for the urban area within the city border is compared to the average for the remaining model domain.

Referring to Table 4, a changing of the albedo of wall and roof surfaces has the strongest effect on urban heat island formation, causing a decrease of UHI in-

tensity by nearly 2 °C. Both vegetation scenarios show a decrease of about 1 °C, similarly to the 'Density' case. The difference in maximum potential temperature between 'Albedo' and 'Control Case' retrieved for the urban area is 2.4 °C. The standard deviation reveals the highest value for the control run, expressing the large differences between impervious and natural surfaces with regard to temperature. Because of insufficient observation data in the rural surrounding, it is difficult to retrieve the UHI inten-

Tab. 4 Impact of scenarios on UHI formation expressed as difference between mean urban and mean rural 2 m potential temperatures. The table also presents the maximum in modeled temperature for the period August 13, 18 UTC as well as standard deviation and mean value of the urban temperatures

Scenario	Albedo	Density	Many Parks	Big Park	Control Case
Θ mean urban [°C]	31.5	32.4	32.5	32.3	33.1
Θ max [°C]	31.9	33.0	33.5	33.3	34.3
Standard deviation [°C]	0.32	0.48	0.50	0.43	0.60
<b>UHI; delta Θ [°C]</b>	<b>0.84</b>	<b>1.32</b>	<b>1.47</b>	<b>1.19</b>	<b>2.52</b>

Tab. 5 Comparison of the planetary boundary layer height for Aug 13 2003 18:00 UTC revealing the biggest effect for the 'Albedo' Scenario; UHII shown by the difference to the rural surrounding

	Albedo	Density	Big Park	Control Case	Rural surrounding
<b>PBLH [m]</b>	584	803	793	1130	565
<b>Delta PBLH [m]</b>	546	327	337		565

sity from measurements. The difference between the 2 m temperatures observed at Stuttgart Schwabenzentrum (37.4 °C) and at Hohenheim University at the urban fringe (33.1 °C) on August 13, 18:00 UTC, is 4.3 °C. Considering the difference in elevation for the two locations (roughly 150 m), the difference is about 3 °C. Another important aspect connected to temperature is the evolution of the planetary boundary layer height (PBLH). This is not discussed in detail here but modelling results retrieved at the location Stuttgart Schwabenzentrum reveal a decrease in PBLH for every scenario (Tab. 5). This decrease correlates with the decrease in temperature; the biggest effect is registered in the ‘Albedo’ scenario. The UHI is also reflected by the difference between PBLH in the urban and in the rural area (Hohenheim). Because of insufficient observation data, validation of the effect of changes in PBLH is not possible at this point, but would be interesting to be pursued in further studies.

To compare the intensity of the various mitigation scenarios over the full modelling period, the difference in 2 m potential temperature between ‘Control Run’ and ‘Scenario Case’ for Stuttgart Schwabenzentrum is given in Figure 9.

The largest impact on 2 m potential temperature for the changed albedo simulation is mostly visible around the solar noon. Urban greening shows the largest impact in the afternoon and evening hours, when the evaporative cooling by the vegetation surface has a greater impact than changed surface reflectivity. Examining a cross-section of 2 m potential

temperature from the northwest to the southeast of the domain, the strength of various mitigation measures can be shown. This cross-section length is about 50 km, covering 50 grid cells of the model domain and passing through the city centre. Here we differentiate between a scenario with white roofs only, and one with roofs and walls modified.

Figure 10 shows the ‘Big Park’ scenario which has the largest impact on air temperature per grid cell. Here a green surface can reduce the temperature by up to 2.5 °C. Changing the albedo for roof surfaces only results in a decrease by about 0.5 °C, whereas by including the walls this effect is more than doubled as there is greater reflection of incoming solar radiation from the urban canopy.

#### 4. Discussion and Outlook

This study simulates a number of urban planning strategies on a regional scale, where the city is treated as a whole system interacting with its surroundings, rather than looking at the street-scale level. With the settings described it is possible to show the effects of various mitigation strategies on UHI formation and urban climate. The conclusions are based on one case study, rather than on a general statistical analysis.

With the chosen parameterisation approach, the model is able to reproduce overall spatial and temporal characteristics of the UHI which are consistent with observations from this and many other studies.

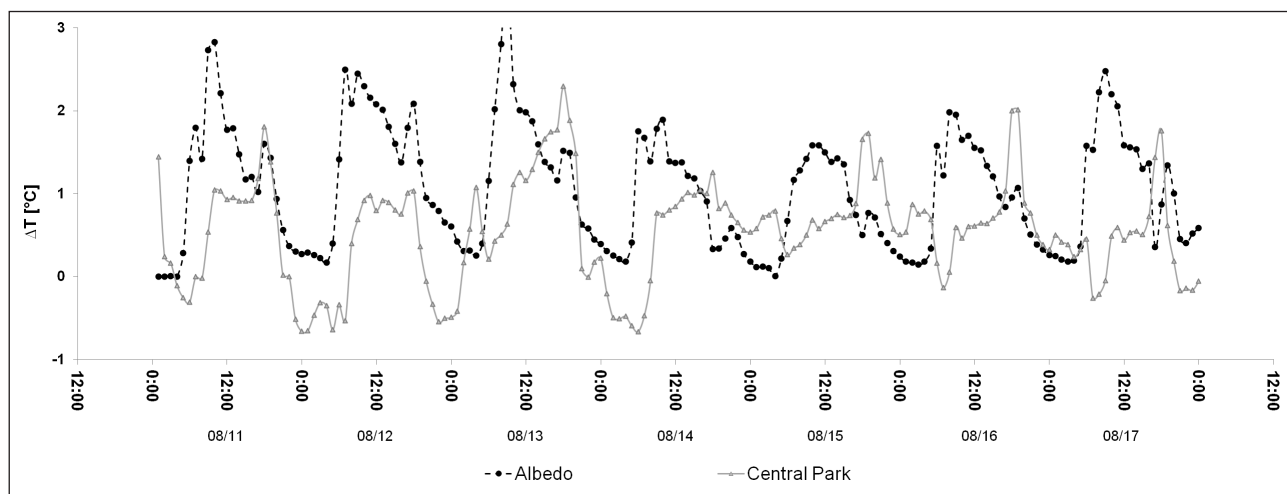


Fig. 9 Difference in 2 m potential temperature between Control Case and the specific urban planning scenario using Building Effect Parameterisation (BEP, Martilli et al. 2002), showing the effectiveness of certain scenario in the course of 7 summer days in 2003 (Aug 11-18)

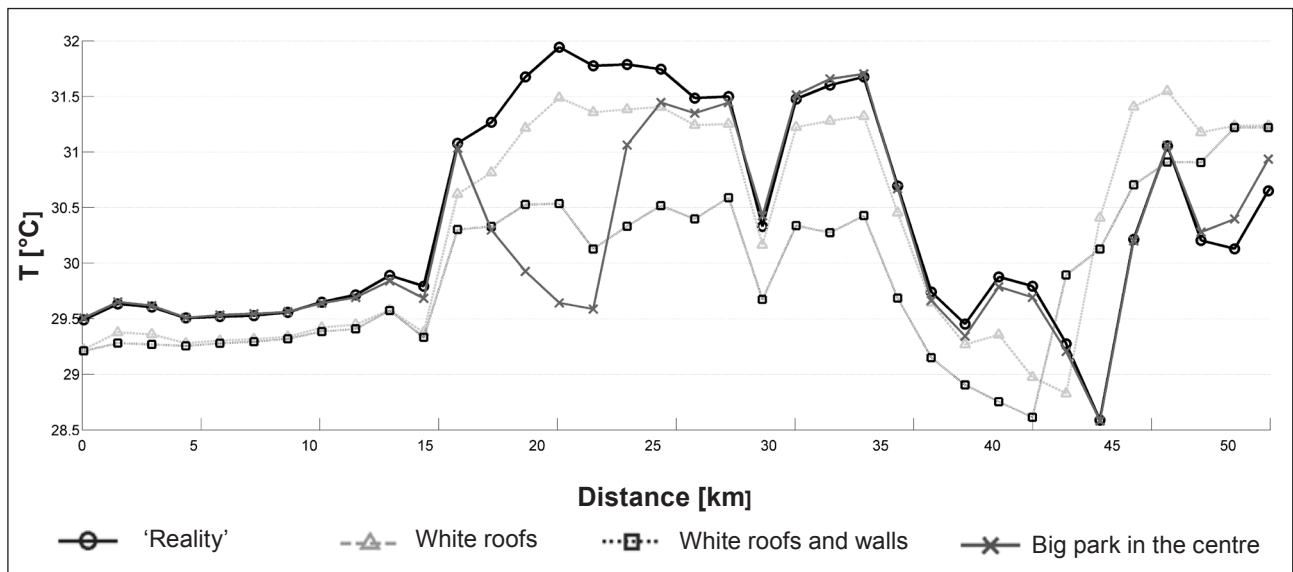


Fig. 10 Cross-section through the city (as given in Fig. 2) of potential 2 m temperature on August 13, 2003, 18:00 UTC; the section from km 15 to km 35 is classified as urban area (Amt für Umweltschutz Stuttgart 2013). For colour code see Fig. 2 (United States Environmental Protection Agency (EPA) 2008).

The scenario with a changed albedo appears to offer the most promising results, reducing the difference in temperature between urban area and rural surrounding by nearly 2 °C, whereas the other strategies – creating green areas and modifying building density – only showed a decrease by about 1 °C, compared to the control case. The temperature maxima are also reduced in all the three scenarios.

Examining the single grid cells, such as in cross-section plots (Fig. 10), grass surfaces tend to have the bigger effect on the 2 m potential temperature regarding one grid cell. For the areal average, the albedo case seems to have the larger impact. The results do not reveal if it is better for city planners to create one big green area in the centre or a diversity of smaller inner city parks.

The general patterns of UHI and temperature reduction through urban planning strategies like those dealt with here can be found in previous studies for various urban areas. Bowler et al. (2010) compared 26 studies assessing the effect of creating green areas in cities, retrieving an average difference in air temperature between a built-up urban area and a green park of 0.5-2.5 °C. Rosenfeld et al. (1998) registered a temperature reduction of combined coloured and vegetated roofs of about 3 °C for the city of Los Angeles, whereas Tong et al. (2005) found a temperature decrease of 1.6 °C for only planting roofs (Rizwan et al. 2008). Taha (1997) reports a 2 °C reduction in UHI intensity as the result of a higher albedo effect, which

is accompanied by a 10 % reduction in energy demand for cooling efforts. Results from the DESIREX 2008 campaign prove that highly reflective roofs were able to reduce the UHI intensity of Madrid significantly, by 1-2 °C (Salamanca et al. 2012).

In our approach, gaining understanding of the impacts of certain mitigation strategies on regional urban-rural interaction is the main goal, rather than street-scale predictions. But still, the results from this kind of studies can provide boundary conditions for smaller-scale urban canopy models.

Simulating the urban heat island in a mesoscale atmospheric model, adapting urban parameterisation schemes, is not new at all, but we have vastly increased the model performance so that the current study is specific to the urban area of Stuttgart and is a basis for discussing the regional scale effects of various measures with local stakeholders.

Another important aspect of urban climate studies is the additional heat production by human activities. This includes increased energy demand for air conditioning during summer periods, and with power plants relying on fossil fuels, air pollutants and greenhouse gas emissions increase. For future work the current modelling approach may also be used for the investigation of the energy saving potential of certain urban planning policies, as well as for further developing the modelling of the energy budget of an urban

area. Furthermore, it is planned to couple the urban canopy model to the chemistry model WRF-Chem, to analyse the effect of the UHI on the formation of pollutants like ozone, NO<sub>x</sub> or aerosols (PM 2.5, PM 10), which again is an important issue concerning human health. So far, this study delivers ideas for specific urban designs to counteract health-related problems like heat stress. For the actual implementation in urban planning, the main result is not to apply one specific mitigation strategy but to apply a mixture of different approaches to reach the best result for a specific geographical area and its inhabitants.

### Acknowledgements

This work is funded by the EU Project “UHI – Development and application of mitigation and adaptation strategies and measures for counteracting the global UHI phenomenon” (3CE292P3) – CENTRAL Europe (2011-2014). The authors also thank the Office for Environmental Protection, Department for Urban Climate, of the City of Stuttgart, the Institute of Environmental Protection of the federal state of Baden-Württemberg, Hohenheim University and the Stuttgart Land Surveying Office for collaboration and access to observation data, as well as the reviewers for their detailed evaluation of the article. We further acknowledge support by Deutsche Forschungsgemeinschaft and Open Access Publishing Fund of Karlsruhe Institute of Technology.

### References

- Akbari, H., S. Bretz, D.M. Kurn and J. Hanford 1997: Peak power and cooling energy savings of high-albedo roofs. – *Energy and Buildings* **25** (2): 117-126
- Akbari, H., S. Menon and A. Rosenfeld 2009: Global cooling: Increasing world-wide urban albedos to offset CO<sub>2</sub>. – *Climatic Change* **94** (3-4): 275-286
- Amt für Umweltschutz Stuttgart 2013: Klimakalender Stuttgart. – Online available at: <http://www.stadtklima-stuttgart.de/index.php?start,02/10/2013>
- Arnfield, A.J. 2003: Two decades of urban climate research: A review of turbulence, exchanges of energy and water, and the urban heat island. – *International Journal of Climatology* **23** (1): 1-26
- Bowler, D.E., L. Buyung-Ali, T.M. Knight and A.S. Pullin 2010: Urban greening to cool towns and cities: A systematic review of the empirical evidence. – *Landscape and Urban Planning* **97** (3): 147-155
- Chen, F., H. Kusaka, R. Bornstein, J. Ching, C.S.B. Grimmond, S. Grossman-Clarke, T. Loridan, K.W. Manning, A. Martilli, S. Miao, D. Sailor, F.P. Salamanca, H. Taha, M. Tewari, X. Wang, A.A. Wyszogrodzki and C. Zhang 2011: The integrated WRF/urban modelling system: Development, evaluation, and applications to urban environmental problems. – *International Journal of Climatology* **31** (2): 273-288
- Chou, M.-D. and M.J. Suarez 1994: An efficient thermal infrared radiation parameterisation for use in general circulation models. – NASA Technical Memorandum 104606, **3**. – Greenbelt, MD
- European Center for Medium-Range Weather Forecasts (ECMWF) 2013: ERA Interim Reanalysis Data. – Online available at: <http://www.ecmwf.int/research/era/do/get/era-interim,02/10/2013>
- Hong, S.Y. and J.O. Jade Lim 2006: The WRF single-moment 6-class microphysics scheme (WSM6). – *Journal of the Korean Meteorological Society* **42** (2): 129-151
- Janjic, Z.I. 1994: The step-mountain eta coordinate model: Further developments of the convection, viscous sublayer, and turbulence closure schemes. – *American Meteorological Society; Monthly Weather Review* **122** (5): 927-945
- Kain, J.S. 2004: The Kain-Fritsch convective parameterization: An update. – *American Meteorological Society; Journal of Applied Meteorology and Climatology* **43** (1): 170-181
- Kusaka, H., H. Kondo, Y. Kikegawa and F. Kimura 2001: A simple single-layer urban canopy model for atmospheric models: Comparison with multi-layer and slab models. – *Boundary-Layer Meteorology* **101** (3): 329-358
- Liu, Y., F. Chen, T. Warner and J. Basara 2006: Verification of a mesoscale data-assimilation and forecasting system for the Oklahoma city area during the Joint Urban 2003 Field Project. – *American Meteorological Society; Journal of Applied Meteorology and Climatology* **45** (7): 912-929
- Luber, G. and M. McGeehin 2008: Climate change and extreme heat events. – *American Journal of Preventive Medicine* **35** (5): 429-435
- Martilli, A., A. Clappier and M.W. Rotach 2002: An urban surface exchange parameterisation for mesoscale models. – *Boundary-Layer Meteorology* **104** (2): 261-304
- Mitchell, K. 2005: The community: Noah land-surface model (LSM). – User's Guide Public Release Version 2.7.1.
- Mlawer, E.J., S.J. Taubman, P.D. Brown, M.J. Iacono and S.A. Clough 1997: Radiative transfer for inhomogeneous atmospheres: RRTM, a validated correlated-k model for the longwave. – *Journal of Geophysical Research: Atmospheres* **102** (D14): 16663-16682
- Oke, T.R. 1982: The energetic basis of the urban heat island. – *Quarterly Journal of the Royal Meteorological Society* **108** (455): 1-24
- Oleson, K.W., G.B. Bonan and J. Feddema 2010: Effects of white roofs on urban temperature in a global climate model. – *Geophysical Research Letters* **37** (3)
- Onishi, A., X. Cao, T. Ito, F. Shi and H. Imura 2010: Evaluating the potential for urban heat-island mitigation

- by greening parking lots. – *Urban Forestry & Urban Greening* **9** (4): 323-332
- Poumadère, M., C. Mays, S. Le Mer and R. Blong* 2005: The 2003 heat wave in France: Dangerous climate change here and now. – *Risk Analysis* **25** (6): 1483-1494
- Rizwan, A.M., L.Y.C. Dennis and C. Liu* 2008: A review on the generation, determination and mitigation of Urban Heat Island. – *Journal of Environmental Sciences* **20** (1): 120-128
- Rosenfeld, A.H., H. Akbari, J.J. Romm and M. Pomerantz* 1998: Cool communities: Strategies for heat island mitigation and smog reduction. – *Energy and Buildings* **28** (1): 51-62
- Salamanca, F., A. Krpo, A. Martilli and A. Clappier* 2010: A new building energy model coupled with an urban canopy parameterization for urban climate simulations – Part 1: Formulation, verification, and sensitivity analysis of the model. – *Theoretical and Applied Climatology* **99** (3-4): 331-344
- Salamanca, F., A. Martilli and C. Yagüe* 2012: A numerical study of the urban heat island over Madrid during the DESIREX (2008) campaign with WRF and an evaluation of simple mitigation strategies. – *International Journal of Climatology* **32** (15): 2372-2386
- Sandvik, B.* 2009: World borders dataset. – Online available at: [http://thematicmapping.org/downloads/world\\_borders.php](http://thematicmapping.org/downloads/world_borders.php), 20/01/2014
- Skamarock, W.C., J.B. Klemp, J. Dudhia, D.O. Gill, D.M. Barker, W. Wang and J.G. Powers* 2005: A description of the advanced research WRF Version 2. – National Center for Atmospheric Research; Technical Note TN-468+STR. – Boulder, Colorado
- Solecki, W.D., C. Rosenzweig, L. Parshall, G. Pope, M. Clark, J. Cox and M. Wiencke* 2005: Mitigation of the heat island effect in urban New Jersey. – *Global Environmental Change Part B: Environmental Hazards* **6** (1): 39-49
- Solomon, S., D. Qin, M. Manning, Z. Chen, M. Marquis, K.B. Averyt, M. Tignor and H.L. Miller* (eds.) 2007: Contribution of Working Group I to the Fourth Assessment Report of the Intergovernmental Panel on Climate Change, 2007. – Cambridge
- Taha, H.* 1997: Urban climates and heat islands: Albedo, evapotranspiration, and anthropogenic heat. – *Energy and Buildings* **25** (2): 99-103
- Tong, H., A. Walton, J. Sang and J.C. Chan* 2005: Numerical simulation of the urban boundary layer over the complex terrain of Hong Kong. – *Atmospheric Environment* **39** (19): 3549-3563
- United Nations (UN) 2011: Urban population, development and environment 2011. – Online available at: [http://www.un.org/esa/population/publications/2011UrbanPopDevEnv\\_Chart/urban\\_wallchart\\_2011-web-smaller.pdf](http://www.un.org/esa/population/publications/2011UrbanPopDevEnv_Chart/urban_wallchart_2011-web-smaller.pdf), 02/10/2013
- United States Environmental Protection Agency (EPA) 2008: Reducing urban heat islands: Compendium of strategies. Urban Heat Island basics. – Online available at: <http://www.epa.gov/hiri/>, 02/10/2013
- USGS 2006: USGS Land Cover Classification. – Online available at: <http://landcover.usgs.gov/pdf/anderson.pdf>, 02/10/2013
- Zhou, Y. and J.M. Shepherd* 2010: Atlanta's urban heat island under extreme heat conditions and potential mitigation strategies. – *Natural Hazards* **52** (3): 639-668